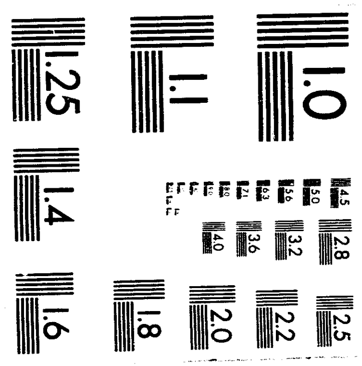
1.0
1.1
1.25
1.4
1.6
1.8
2.0
2.2
2.5
2.8
3.2
3.6
4.0
4.5
5.0
5.6

DOE/ER/61066--T3

Development of a Radiative Cloud Parameterization Scheme of Stratocumulus and Stratus Clouds Which Includes the Impact of CCN on Cloud Albedo

William R. Cotton
Colorado State University
Dept. of Atmospheric Science
Fort Collins, Colorado

January 18, 1994

1 Objectives:

The objective of this research is to develop a parameterization scheme that is able to diagnose or predict changes in stratocumulus cloud cover, atmospheric boundary layer (ABL) stability, liquid water paths (LWPs), and cloud albedo due to changes in sea-surface temperatures, large scale vertical motion and wind shear, and cloud condensation nuclei (CCN).

The motivation for developing such a parameterization scheme is that it is hypothesized that anthropogenic sources of CCN can result in increased concentrations of cloud droplets (Twomey, 1977: Schwartz, 1988). The higher concentrations of CCN result in higher concentrations of cloud droplets, thereby enhancing cloud albedo which in the absence of other effects will induce a climate forcing opposed to that associated with 'Greenhouse' warming (Charlson, 1992).

While this hypothesis is quite simple, there are a number of complicating issues that we are examining. These are:

(i) Sub-cloud CCN have a direct influence on cloud droplet concentrations and droplet spectra near cloud base, but many other factors such as entrainment of CCN in the stable inversion, droplet spectral broadening by turbulence, collection, and the presence of ultra-giant nuclei, determine the droplet spectra through the greater depth of the cloud.

(ii) The residence time of aerosol in the boundary layer is relatively short. Thus, the most likely location of anthropogenic aerosol that can potentially affect cloud microstructure is immediately above the capping inversion. As a result, the effects of these aerosol on boundary layer clouds is dependent upon the entrainment into the boundary layer.

(iii) Cloud radiative properties are primarily controlled by cloud liquid water path and only clouds of modest or small liquid water paths are susceptible to modest changes in droplet concentrations.

(iv) Cloud radiative properties are also complicated functions of cloud geometry such as inhomogeneities in the cloud top geometry and inhomogeneities in the internal cloud macrostruction. Such inhomogeneities can make a cloud appear much less reflective than 'idealized' flat cloud tops thus masking the impacts of enhanced CCN concentrations.

As a result of the complicated interactions between cloud microstructure, cloud macrostructure, and cloud radiative transfer, only a limited range of clouds are susceptible to changes in CCN concentrations causing changes in cloud albedo. It is the intent of this research to determine the range of cloud types that are susceptible to albedo changes by anthropogenic CCN and incorporate that information into a cloud parameterization scheme.

2 Results:

As part of this research, a detailed explicit cloud physics model developed at the University of Tel-Aviv (Tzivion et al., 1987; Feingold et al., 1988; Tzivion et al., 1989) has been implemented in RAMS. This scheme was selected because of its inherent accuracy in representing the evolution of droplet spectra due to condensation and collection. This accuracy is achieved by conserving two or more moments of the droplet spectra (e.g., number density and mass mixing ratio). Thus, this model with 25 bins in the droplet spectra has the accuracy equivalent to or greater than a 50+ bin model conserving only droplet number density.

The interfacing of the LES model and the explicit microphysics models has been completed with the results of preliminary two-dimensional simulations reported by Feingold et al. (1993). The results of the first three-dimensional simulation with the model were described at an invited paper at the ECMWF/GCSS workshop in Reading, England (Cotton et al., 1993). The results and analysis of our second three-dimensional simulation are described by Stevens et al. (1994).

Some of the refinements in the latest version of the LES/explicit microphysics (EM) are as follows.

2.1 Activation

The activation process, which describes the transition of hygroscopic aerosols into cloud drops, has been developed in terms of a multi-bin model where a distribution is assumed within each bin such that the initial activation profile matches that reported (Hudson and Frisbie, 1991) from observations made during FIRE I.

2.2 Advection Schemes

A new advection scheme was implemented in the model. Advective errors tended to degrade our solutions in the vicinity of cloud top, causing high supersaturations, oscillations in the liquid water mass and drop concentration fields. This situation is commonly encountered in numerical cloud models (Grabowski, 1989). Since these are generally just single grid point features, they are not considered a problem in most LES models. In our project, however, local enhancements of liquid water content and droplet concentrations can affect our cloud albedo calculations to the extent that they mask the physical solutions of the model.

To rectify this situation we experimented with monotonic flux corrections to our higher-order advection schemes (Smolarkiewicz and Grabowski, 1990). The results were encouraging and the methodology was introduced into the model. In two dimensions we found the results were sensitive to how much diffusion was added by the flux correctors to combat the non-monotonic tendencies of the higher order schemes. The best results were associated with the peak preservers of Zalesak (1979) unfortunately this was the most computationally demanding approach as well. We proceeded with this form of flux correction, however, since the more diffusive scheme artificially degraded our inversion thereby promoting artificially high entrainment velocities, and artificially low liquid water contents. The model was run in 3-D with the new advection schemes, which greatly improved results.

2.3 Radiation parameterization in RAMS

Previously the upper boundary condition for the radiation parameterization in RAMS was the top of the model domain. This resulted in too little downward longwave radiation at cloud top and too much impinging solar radiation. The radiation code was modified to include the rest of the troposphere for the purpose of radiation calculations. The above-model-top part of the troposphere does not interact dynamically with the rest of the model. Thermodynamic, and moisture profiles were interpolated from the NGM analysis files using RAMS in a meso-scale configuration.

2.4 Regeneration schemes

We found that the model was sensitive to how we distributed the CCN returned after a droplet evaporated. Originally we were returning CCN in accordance with the initial distribution, this led to a conversion of large CCN to small CCN. By altering the regeneration scheme so that the overall distribution of CCN was forced toward the initial distribution (a more physical scenario) we found our results to be much steadier.

2.5 Nested gridding in droplet mass space

During the course of our work over the past year it has become clear that the overhead (CPU and memory) associated with the detailed bin model are significant. The current microphysical configuration requires an additional 56 scalar variables (50 for the drop spectrum and 6 for the CCN spectrum) and the associated microphysical calculations are quite intensive. Because use of a bulk microphysical scheme (which predicts only cloud water content) would not be adequate for the purpose of this study, we have proposed the idea of using a nested gridding in the *mass domain.* This idea is borrowed from the concept of nested gridding in the *spatial domain* which is a feature of RAMS and other cloud and mesoscale models. The main idea behind nested gridding for droplet mass is that we do not always need, or, may not always be able to afford, great microphysical detail. Nested gridding in mass space offers the choice of maximum resolution of drop size in the areas of cloud (or stages of cloud evolution) where it is most necessary, and coarser resolution where (or when) it is less important.

In order to implement the idea of nested gridding in the mass domain, two steps were necessary. The first was the extension of our moment based microphysical treatment to coarser resolutions. This work has been performed by our collaborators at the Tel Aviv University. The second step required the ability to map drop spectra from fine resolution mass grids to coarse resolution grids and vice versa. This has been achieved using moment conserving interpolation functions. Initial experiments which implement this nested gridding technique are now underway. During the coming months we will continue to test these schemes in various configurations in order to evaluate their effectiveness. It is hoped that this technique will allow a more effective use of computing resources and free computer time and memory when high resolution in mass space is not imperative.

2.6 Simulations

Two three dimensional and scores of two dimensional simulations have been carried out. The 2-D simulations were conducted to give us a sense of the sensitivity of the model to activation, and regeneration parameterizations. As well, we looked at the effect of varying subsidence rates and differing advective schemes on the model configured in 2-D. The latter three dimensional run is being analyzed at this moment. In particularly, the layer is buoyantly- driven and an analysis of the fluxes and thermodynamic fields compare favorable with other published results, as do entrainment velocities and velocities scales. We have fixed the problem of the drying out above cloud top which was identified by Moeng and Deardorff in their simulations. We have also found that negative fluxes of total moisture found in previous stratocumulus LESs above cloud top are artifacts of non-monotonic advection schemes.

Figure 1 shows a surface of $0.02 g/kg$ liquid water mixing ratio which Noonkester (1984) defined as cloud edges. We have plotted this surface to demonstrate the 3-Dimensional variability of the clouds. We expect fluxes of drizzle to contribute significantly to the variability of these clouds, and believe that this approach to modelling (LES-EM) will provide us an important tool in assessing to what extent the full three dimensional structure is important in maintaining the energy and moisture budgets of the layer. Note the exceedingly ragged cloud base structure, and evidence of penetrating cumulus (with overshooting tops) associated with more vigorous updrafts.

Figure 2 is a scatter plot of the total water in the model plotted at the different model vertical levels. Superimposed is a line representing the horizontal average total water as a function of height. Total water is a good example of a field which is well mixed in the boundary layer and nearly discontinuous across the inversion.

Shown in Figure 3 are vertical profiles of the horizontally averaged liquid water. Conditional sampling was used to distinguish regions where $w > 25\ cms^{-1}$, these regions are identified as updrafts. In a similar sense downdraft averages were identified. Liquid water was averaged over these regions and is included in the plot. Also we calculated an adiabatic liquid water profile and included this as a dotted line. Adiabatic profiles of liquid water were difficult to determine since selection of cloud base was poorly defined. The characteristic raggedness of cloud base in these simulations represents a feature of these types of clouds which our modelling methodology (LES-EM) is particularly well equipped to handle. The layer average profiles of liquid water are sub-adiabatic as are expected for stratus clouds, although we found updraft cores to be adiabatic in our analysis, with super adiabatic regions near cloud top. Super adiabatic profiles in these cores were found to result

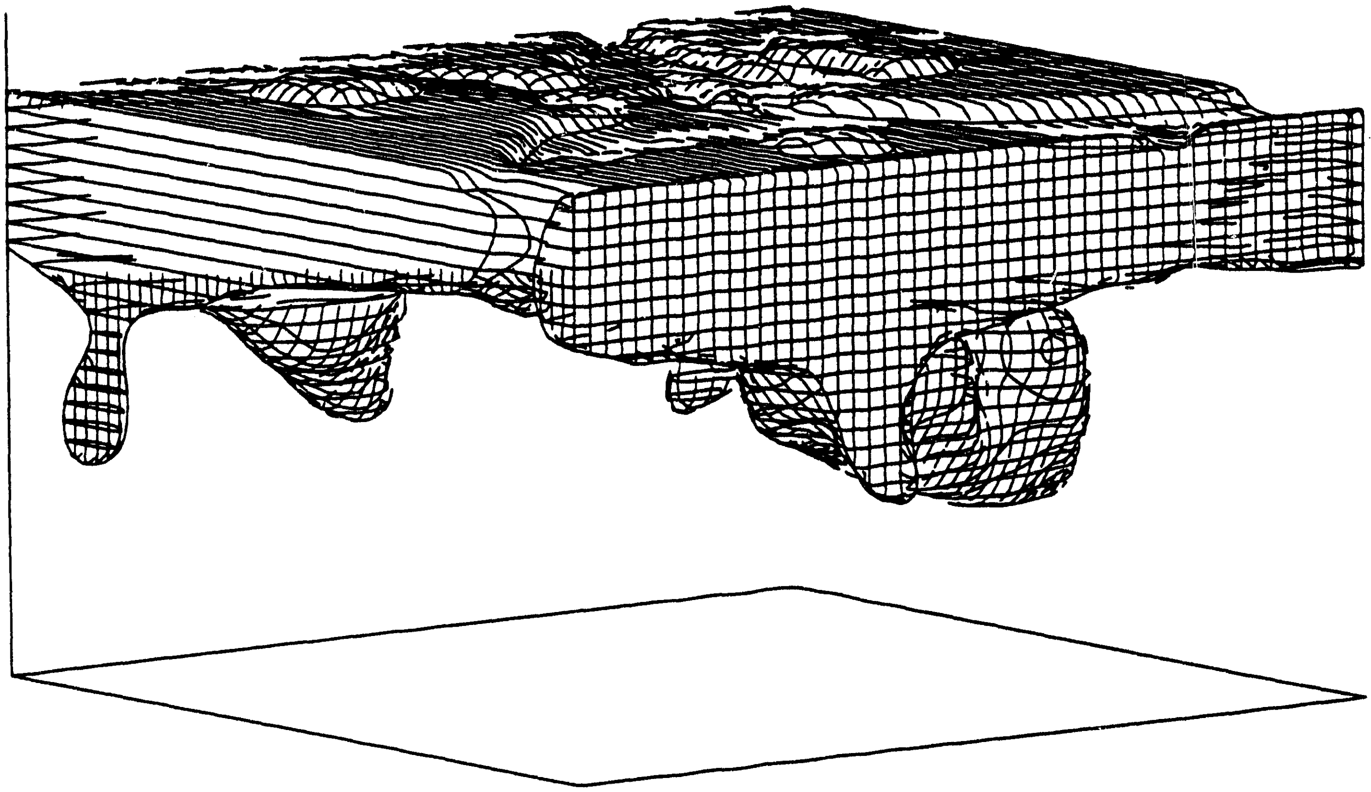

Figure 1: Plot of $0.02g/kg$ liquid water surface.

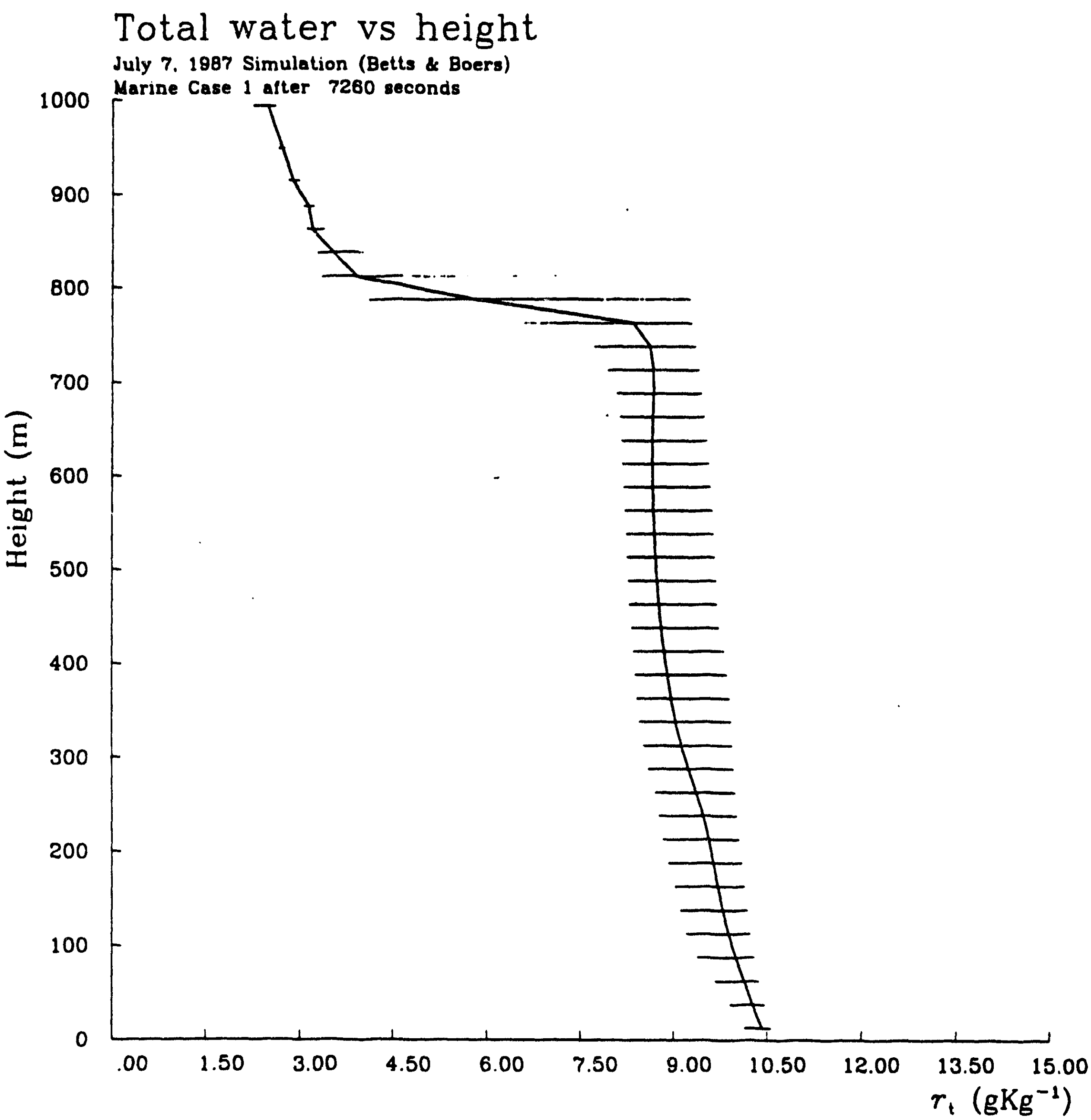

Figure 2: Total water mixing ratio (gkg^{-1}) plotted at the various model levels. Horizontal lines are actually scatter plots of the value of total water at each point across a given horizontal level. Profile represents a line drawn through the average total water at each level.

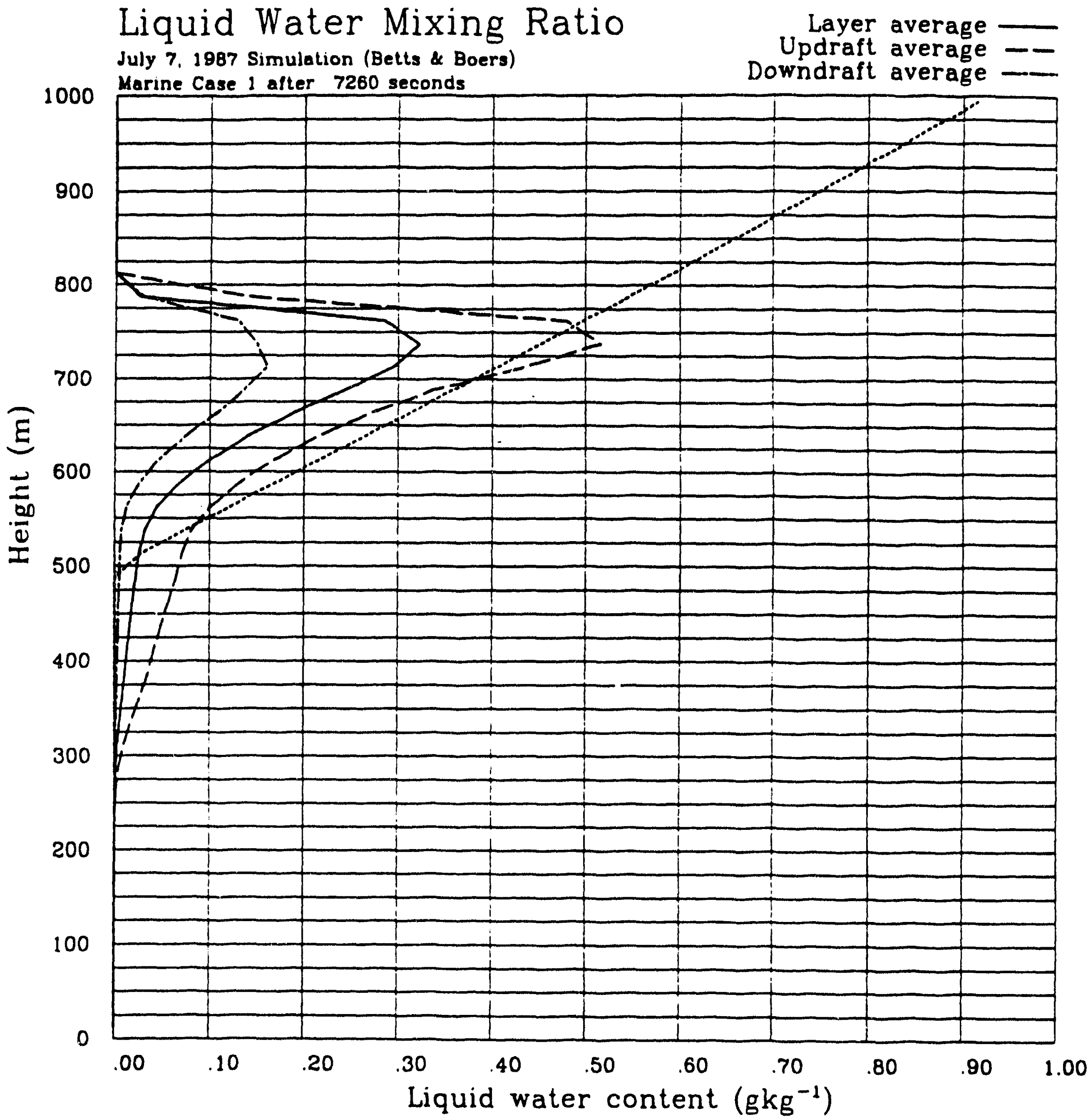

Figure 3: Vertical profiles of liquid water content (gm^{-3}). Updraft averages taken over regions where $w > 25\ cms^{-1}$, while downdraft averages were taken over regions where $w < 25\ cms^{-1}$. Adiabatic liquid water profiles were plotted as a function of height assuming a certain level for cloud base.

from longwave cloud top cooling. An experiment in which higher concentrations of CCN have been introduced above the capping inversion has also been completed. Results of that run are currently being analyzed.

2.7 Radiation diagnostic model

The model is based on the Spherical Harmonic Spatial Grid (SHSG) method, and is described in Evans (1993). This method discretizes the radiative transfer equation by expanding the angular part of the radiance field in a spherical harmonic series and representing the spatial part of the radiance field on a discrete grid. The method is generally faster than other general multi-dimensional RTMs, making it feasible for both monochromatic and broad band calculations. The model also has an independent pixel mode (I.P.) where the horizontal coupling of the radiative terms are eliminated, resulting in a plane-parallel version of the model.

In the broadband version of the SHSG model, molecular absorption is modeled using broad band k distribution data from K. -D. Chou and the ozone cross section data of Stamnes and Tsay (1990). The absorbing gases included in the solar model are H_2O, CO_2, O_2 and O_3. Rayleigh scattering is also included.

The SHSG model, like LES/EM model, is computationally intensive. In order to make broadband calculations possible, narrow band (20 cm^{-1} to 50 cm^{-1}) k distribution data were summed into 14 bands in the solar wavelength region (.28 - 3.8 microns) and 10 bands in the longwave region (3.8 - 500 microns). In each band, the number of weights in the k-distribution function were reduced to nine by averaging the weights across the k (absorption coefficient) space (Chou, 1986). Chou and Arking (1981) have found that broadband heating rate computations remain accurate when the number of weights is reduced to approximately ten.

In the SHSG model, the resolution of the discrete grid must be fine enough to adequately approximate the spatial derivatives in the radiative transfer equation. Experimentation has shown that for inhomogeneous atmospheres, the optical path across an individual grid cell must not be greater than roughly one in order to give accurate results. In the k-distribution method the optical paths associated with the largest k's are so large that the grid required for such a calculation is well beyond the capacity of current computers. In order to surmount this problem, an alternative plane-parallel solution method is used when the optical paths exceeds our computational capacity. The errors associated with the plane-parallel solution in these cases are negligible.

The microphysical properties derived from two 2D RAMS simulations were used in a test of the radiative transfer model. One set of simulations used a typical maritime CCN concentration of 100 cm^{-3} (Case N) and the second used an enhanced CCN concentration of 500 cm^{-3} (Case O). Cloud optical properties were derived from Mie scattering solutions of the particle size distributions given from the RAMS simulations. The asymmetry parameters calculated for each band were used as g_{eff} in the double Henyey-Greenstein (HG) phase function in order to approximate the phase function. The double HG has the form, $P(cos\Theta) = bP(g_1) + (1-b)P(g_2)$, where in both simulations $g_1 = g_{eff} + 0.05$, $g_2 = -0.6$, and b is a variable related by $g_{eff} = bg_1 + (1-b)g_2$. The optical properties of the atmosphere were calculated by scaling the optical properties of the cloud, the gases and Rayleigh scattering (Slingo and Schrecker, 1982, Liou and Sasamori, 1975).

The spectral fluxes at the top of the radiative transfer model were calculated from LOWTRAN 7 using a composite sounding of interpolated NWS data and the initial sounding from Betts and Boers (1990) in the lowest 15 km, and the summer midlatitude atmosphere from the LOWTRAN 7 model above 15 km.

Calculations of the visible (0.4 - 0.7 μm) cloud top albedos for both cases at three solar zenith angles show that cloud albedo is closely related to the cloud liquid water path and zenith angle (Stephens, 1978). The albedos computed from the 2D simulations in the high sun runs were generally within less than two percent of the IP calculations at each point along the horizontal domain, except in regions of the cloud where the liquid water path changes rapidly. The effect of the 2D calculations was to smooth out the albedo field compared with the IP results. These results are in contrast to earlier radiance calculations of the same cloud fields that showed large differences in the reflected radiances from the 2D and IP runs at viewing angles far from nadir; the reflected fluxes show much smaller differences. The albedo differences between the 2D and IP calculations in the low sun runs were only slightly larger. It should be noted, however, that horizontal variability of the cloud fields in the 2D simulations were, in general, not large and the albedos from more broken cloud fields may be more significantly affected by cloud geometry.

A comparison of the albedos from Case N and Case O show the enhanced CCN in Case O appeared to affect the broad band albedo mostly through the resulting microphysical changes. The smaller droplet sizes and larger liquid water paths resulted in an average increase of 7.5 percent in the domain-averaged cloud albedo in the enhanced CCN simulations.

The results of broadband flux convergence calculations in the near infrared also show the limited impact of horizontal inhomogeneities on cloud radiative fluxes. In general, the effects of gaseous absorption tended to help drown out the radiative differences from horizontal transport, and the relative differences between the 2D and plane parallel flux convergence were less than the relative differences in cloud albedo.

Monochromatic and solar broadband calculations of the radiative transfer are currently in progress using the microphysical properties derived from the 3D RAMS simulations. Preliminary results suggest that the differences between the 2D radiative transfer model calculations and the one dimensional IP calculations are slightly larger than the differences in the previous test with the 2D RAMS data. Radiative transfer calculations of a cloud field from the 2D RAMS simulation and a 3D RAMS simulation with a similar (but not identical) CCN concentration are shown below. In both simulations, the solar zenith angle is 10 degrees and the albedos are from the visible wavelengths (0.4 to 0.7 microns).

	Domain mean albedo	Standard deviation
2D RAMS cloud (2D SHSG)	0.316	0.104
2D RAMS cloud (IP)	0.317	0.112
3D RAMS cloud (2D SHSG)	0.358	0.103
3D RAMS cloud (IP)	0.363	0.137

In both sets of simulations the albedo field from the 2D radiative transfer model calculations are smoother compared to the corresponding IP albedo field. The IP model calculations also suggest that the 3D RAMS runs produced more of an optically inhomogeneous cloud (because of the larger standard deviation). This may account for the slightly larger difference in the domain average cloud albedo in the new set of calculations (0.1 percent compared to 0.5 percent). However, for stratified clouds, the impact of geometry effects on broadband albedo still appear to be limited.

In addition to the above radiative calculations, the LES/EM model output was sent to Professor Peter Jonas of the University of Manchester (UMIST) England where his group is using a Monte Carlo radiation code to calculate cloud albedo.

3 References

Betts, A.K., and R. Boers, 1990: A cloudiness transition in a marine boundary layer. *J. Atmos. Sci.*, **47**, 1480-1497.

Charlson, R.J., S.E. Schwartz, J.M. Hales, R.D. Cess, J.A. Coakley, Jr., J.E. Hansen, D.J. Hofmann, 1992: Climate forcing by anthropogenic aerosols. *Science,* **255,** 423-430.

Chou, M. -D., 1986: Atmospheric solar heating rate in the water vapor bands. *J. Clim. Appl. Meteor.,* **25,** 1532-1542.

Chou, M. -D., and A. Arking, 1981: An efficient method for computing the absorption of solar radiation by water vapor. *J. Atmos. Sci.,* **38,** 798-807.

Cotton, William R., Bjorn Stevens, Graham Feingold, and Robert L. Walko, 1993: Large Eddy Simulation of Marine Stratocumulus Cloud with Explicit Microphysics. *Proc., ECMWF/GCSS Workshop on Parameterization of the Cloud Topped Boundary Layer,* Reading, United Kingdom, 8-11 June 1993.

Evans, F., 1993: Two-dimensional radiative transfer in cloudy atmospheres: The spherical harmonic spatial grid method. *J. Atmos. Sci.*, **50**, 3111-3124.

Feingold, G., S. Tzivion, and Z. Levin, 1988: Evolution of raindrop spectra. Part I: Solution to the stochastic collection/breakup equation using the method of moments. *J. Atmos. Sci.*, **45**, 3387-3399.

Feingold, Graham, Bjorn Stevens, William R. Cotton, Robert L. Walko, 1993: An explicit cloud microphysics/LES model designed to simulate the Twomey effect. Accepted *J. Atmos. Res.*

Grabowski, Wojciech W., 1989: Numerical Experiments on the dynamics of the cloud-environment interface: small cumulus in a shear free environment. *J. Atmos. Sci.*, **46**, 3513-3541.

Hudson, J.G., and P.R. Frisbie, 1991: Cloud condensation nuclei near marine stratus. *J. Geophys. Res.*, **96**, 20,795-20,808.

Liou, K. N., and T. Sasamori, 1975: On the transfer of solar radiation in aerosol atmospheres. *J. Atmos. Sci.*, **32**, 2166-2177.

Noonkester, V.R., 1984: Droplet Spectra Observed in Marine Stratus Cloud Layers. *J. Atmos. Sci.*, **41**, 829-844.

Schwartz, S.E., 1988: Are global cloud albedo and climate controlled by marine phytoplankton? *Nature*, **336**, 441-445.

Slingo, A., and H. M. Schrecker, 1982: On the shortwave properties of stratiform water clouds. *Q. J. Roy. Meteorol. Soc.*, **108**, 407-426.

Smolarkiewicz, Piotr K., and Wojciech W. Grabowski, 1990: The multidimensional positive definite advection transport algorithm: nonoscillatory option. *J. Comput. Phys.,* **86,** 355-375.

Stamnes, K., and S. -C. Tsay, 1990: Optimum spectral resolution for computing atmospheric heating and photodissociation rates. Planet. Space Sci., 38, 807 - 820.

Stephens, G. L., 1978: Radiative properties of extended water cloud . II: Parameterizations. J. Atmos. Sci., 35, 2123 - 2132.

Stevens, B., W.R. Cotton, G. Feingold, R.L. Walko, 1994: Large eddy simulations of marine stratocumulus with explicit microphysics. Proc., 8th Conf. on Atmospheric Radiation, 23-28 January 1994, Nashville, TN, AMS.

Twomey, S., 1977: The influence of pollution on the shortwave albedo of clouds. *J. Atmos. Sci.,* **34,** 1149-1152.

Tzivion, S., G. Feingold, and Z. Levin, 1987: An efficient numerical solution to the stochastic collection equation. *J. Atmos. Sci.,* **44,** 3139-3149.

Tzivion, S., G. Feingold, and Z. Levin, 1989: The evolution of raindrop spectra. Part II: Collisional collection/breakup and evaporation in a rain shaft. *J. Atmos. Sci.,* **46,** 3312-3327.

Zalesak, Steven T., 1979: Fully multidimensional flux-corrected transport algorithms for fluids. *J. Comput. Phys.,* **31,** 335-362.

DATE FILMED

5/5/94

END